SIMULATION OF AN INTEGRATED HYDROGEN FUEL CELL WITH LIBR-WATER ABSORPTION SYSTEM FOR COMBINED PRODUCTION OF ELECTRICITY, COOLING AND HOT WATER

Sieres J.* and Martínez-Suárez J.A.
*Author for correspondence
Área de Máquinas y Motores Térmicos,
Escuela de Ingeniería Industrial, Campus Universitario Lagoas-Marcosende, University of Vigo,
Vigo, 36310,
Spain,
E-mail: jsieres@uvigo.es

ABSTRACT

In this paper, a computer simulation was performed to analyze the integration of a hydrogen solid oxide fuel cell (SOFC) with a LiBr-water absorption system, for the simultaneous production of electricity, cooling and hot water. The exhaust gases from the SOFC are used to power the generator of the absorption system, where cooling is obtained, and also to produce hot water in a heat exchanger. For the purpose of enhancing the energy utilization efficiency of the system, heat exchangers are also used to preheat the reactant streams of the SOFC with the exhaust gases. A steady state mathematical model was developed to simulate the performance of the whole system under different operating conditions. The performances of the integrated energy system and of the different subsystems are evaluated under different operating conditions. Especially, the effect of the absorption system generation temperature was scrutinized in order to determine optimum operating conditions.

NOMENCLATURE

CAT	[K]	Closest approach temperature
COP		Coefficient of performance
EFF	[-]	Heat exchanger efficiency
g	[kJ/kmol]	Specific Gibbs free energy
h	[kJ/kmol]	Specific molar enthalpy
HHV	[kJ/kmol]	Higher heating value
$\dot{N}$	[kmol/s]	Molar flow
PER		Primary energy ratio
$\dot{Q}$	[kW]	Heat power
s	[kJ/ kmolK]	Specific molar entropy
$\dot{S}_g$	[kW/K]	Rate of entropy generation due to irreversibility's
T	[ºC, K]	Temperature
$\dot{W}$	[kW]	Electrical power

Special characters
η	[-]	Efficiency

Subscripts
A	Absorber
C	Condenser
E	Evaporator
eq	In equilibrium
fc	Fuel cell
G	Generator
hw	Domestic hot water
in	Carried into the fuel cell
l	Liquid
out	Taken out of the fuel cell
P	Pump
ss	Strong solution
v	Vapor
ws	Weak solution

INTRODUCTION

Today's concerns regarding fossil fuels contribution to environmental pollution call for the utilization of new efficient energy systems and energy conversion processes compatible with alternative fuels and renewable energy sources and carriers. Under this scenario, fuel cells and hybrid systems have emerged as promising thermodynamic systems for achieving all of the above requirements. In fact, fuel cells are absolutely zero emission devices when fuelled with pure hydrogen, with the only by-product being water vapor [1].

In a fuel cell, the chemical energy of a fuel and an oxidant is converted directly into electrical energy. Although fuel cells are not heat engines, heat is still produced and must be removed from a fuel cell power system. Various types of fuel cells are available, differentiated by the electrolyte used which, in turn, depends on its operating temperature. Solid oxide fuel cells (SOFC) are high temperature fuel cells that consist of a solid oxide metal electrolyte (typically yttria stabilized zirconia). At the anode nickel cermet is usually used, while the cathode is made of strontium doped with lanthanum manganite.

SOFCs have been identified as promising power generator devices due to their high electrical efficiencies. Moreover, since SOFCs operate in the range of 600 to 1000 ºC, they can be easily combined with other thermal cycles to yield improved thermal efficiencies.

Though actual research efforts are focused on single cells and stack operation, simulations of global systems for the simultaneous production of power, cooling and/or heating from a fuel cell are crucial to find optimal design and operating conditions. Studies similar to the type of integration system considered in this paper have been reported in Refs. [2-6].

This paper presents results of a thermodynamic analysis of the integration of a hydrogen solid oxide fuel cell (SOFC) with a LiBr-water absorption system, for the simultaneous production of electricity, cooling and hot water. A steady state mathematical model was developed to simulate the performance of the whole integrated energy system and of the different subsystems. The effects of the absorption system generation temperature and heat power were scrutinized in order to determine optimum operating conditions.

CONFIGURATION AND DESCRIPTION OF THE INTEGRATED SYSTEM

Figure 1 shows a schematic representation of the integrated energy system. It consists of a hydrogen solid oxide fuel cell (SOFC), a LiBr-water absorption system and three heat exchangers (H_2, air and domestic hot water). The system can simultaneously produce electricity, cooling and hot water.
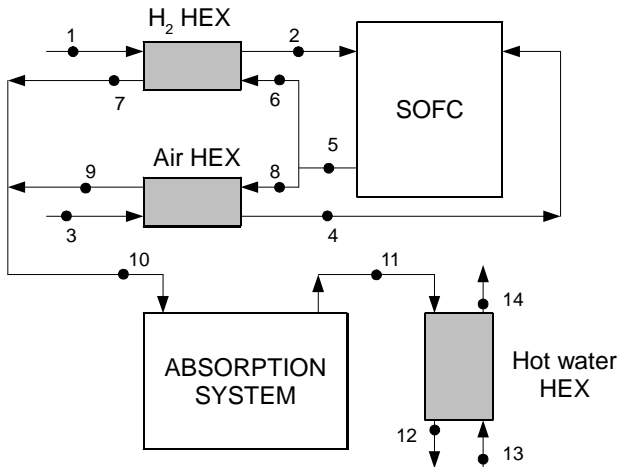

Figure 1 Schematic representation of the integrated system.

The operating principle of the integrated system can be summarized as follows. The SOFC's fuel, pure H_2, is preheated through the heat exchanger (H_2HEX) and fed into the SOFC anode. Similarly air is preheated in the heat exchanger (AirHEX) and fed into the SOFC cathode. In the SOFC, the chemical energy of the fuel (H_2) and the oxidant (O_2 in the air) is converted into electrical energy and heat. The high temperature exhaust gases from the SOFC are used to preheat the reactants streams to the SOFC in order to improve the

thermodynamic efficiency of the SOFC. Then, the exhaust gases are used to power the generator of the absorption chiller, where cooling is obtained. Finally, the exhaust gases leaving the generator are used to produce hot water in a heat exchanger.

The single effect LiBr-water absorption system being considered is depicted schematically in Figure 2. The absorption system uses the pair lithium bromide-water and its major components are the absorber, generator, condenser, evaporator, solution heat exchanger, pump and two expansion devices. The generator is powered with the hot exhaust gases from the SOFC (stream 10 and 11 in Figure 1 and streams 11 and 12 in Figure 2). Water is used as the external cooling medium in the absorber and condenser. Finally, cold water is produced in the evaporator for the typical temperature levels found in air-conditioning systems.
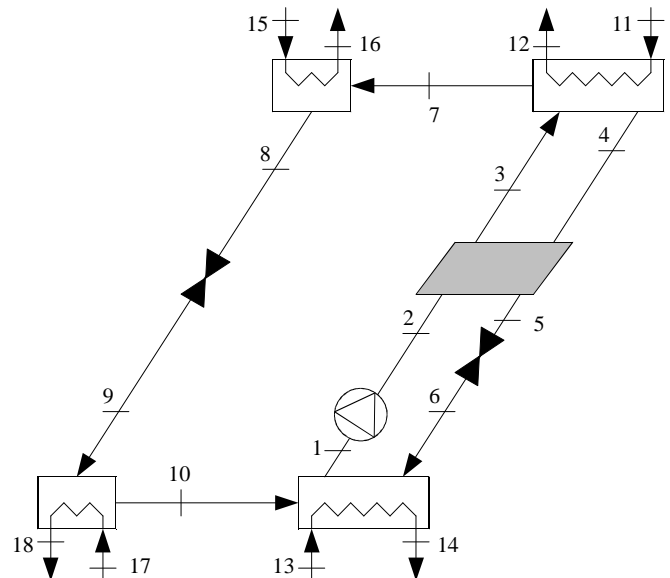

Figure 2 Schematic representation of the absorption system.

SYSTEM MODELLING

A lumped steady state model has been developed in order to analyze the performance of the integrated energy system. A lumped parameter model considers a component as a lump or a black box, so the actual dimensions of the components and detailed transport processes inside them are not taken into account. These types of models are appropriate for the present analysis since attention is not focused on the fuel cell itself or the absorption system components, but rather on how the operating conditions affect the performance of the whole system.

The mathematical model of the integrated system is based on the application of global mass, species, energy balances and simple heat and mass transfer equations. The following general assumptions have been considered for the whole system: the system operates at steady-state conditions, pressure drops are negligible except in the pumps and expansion devices, the heat transfer between the exchangers and the surroundings is negligible, the SOFC's fuel consists of pure H_2 at atmospheric

conditions, the atmospheric air that enters the SOFC consists of 79% N_2 and 21% O_2, reactants and products of the SOFC can be considered as ideal gases and their enthalpy and entropy values are based on JANAF table references [7]. It is also assumed that the values of the product gases flow rates through each of the heat exchangers (H_2HEX and AirHEX) are those for which the temperature of the reactants at the inlet of the SOFC is the same (i.e. $T_2 = T_4$).

In the following sections the mathematical models for the SOFC and absorption system are detailed. The performance of the hot water heat exchanger is defined based on its effectiveness in terms of temperatures:

$$EFF_{hw} = \frac{\max(T_{11}-T_{12}, T_{14}-T_{13})}{T_{11}-T_{13}} \tag{1}$$

SOFC model

The SOFC is modeled as a control-volume system to which fuel and oxidant streams enter and product gases exit. The basic assumptions for the SOFC are: the SOFC operates at steady-state conditions, the pressure is constant, an ideal and complete stoichiometric reaction takes place, the fuel cell is located inside a thermal bath in order to maintain the desired operating temperature, the outlet gas temperatures are equal to the SOFC temperature, all heat transfer between the cell and its surroundings occurs through boundaries at the temperature of the fuel cell, the kinetic and gravitational potential energy changes are negligible, and the SOFC operates under thermodynamically reversible condition so the rate of entropy generation due to irreversibility's is zero.

The electrochemical reaction that occurs within the anode and cathode of the solid oxide fuel cell is described as follows:

$$H_2 + 2.381 \cdot (0.21 \cdot O_2 + 0.79 \cdot N_2) \rightarrow$$
$$H_2O + 1.881 \cdot N_2 + \dot{Q}_{fc} + \dot{W}_{fc} \tag{2}$$
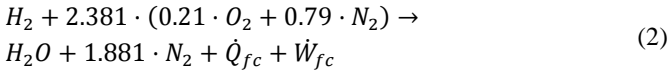
where $\dot{W}_{fc}$ is the rate of work done by the fuel cell and $\dot{Q}_{fc}$ is the rate of heat transferred into the fuel cell from the surroundings.

Taking into account the previous reaction and the assumptions considered, the first and second law of thermodynamics can be written as [8]:

$$\dot{N}_{H_2} \cdot h_{H_2}\big|_{in} + \dot{N}_{O_2} \cdot h_{O_2}\big|_{in} + \dot{N}_{N_2} \cdot h_{N_2}\big|_{in}$$
$$-\dot{N}_{H_2O} \cdot h_{H_2O}\big|_{out} - \dot{N}_{N_2} \cdot h_{N_2}\big|_{out} + \dot{Q}_{fc} - \dot{W}_{fc} = 0 \tag{3}$$

$$\dot{N}_{H_2} \cdot s_{H_2}\big|_{in} + \dot{N}_{O_2} \cdot s_{O_2}\big|_{in} + \dot{N}_{N_2} \cdot s_{N_2}\big|_{in}$$
$$-\dot{N}_{H_2O} \cdot s_{H_2O}\big|_{out} - \dot{N}_{N_2} \cdot s_{N_2}\big|_{out} + \frac{\dot{Q}_{fc}}{T_{fc}} + \dot{S}_g = 0 \tag{4}$$

where $\dot{N}$ is the molar flow rate, h is the specific molar enthalpy, s the specific molar entropy, T_{fc} is the fuel cell absolute temperature and $\dot{S}_g$ is the rate of entropy generation due to irreversibility's.

The previous equations can be simplified as:

$$\dot{N}_{H_2} \cdot (h_{in} - h_{out}) + \dot{Q}_{fc} - \dot{W}_{fc} = 0 \tag{5}$$

$$\dot{N}_{H_2} \cdot (s_{in} - s_{out}) + \frac{\dot{Q}_{fc}}{T\_fc} - \dot{S}_g = 0 \tag{6}$$

where h_{in} is the amount of enthalpy per mole of H_2 carried into the system by the reactant inflow and h_{out} is the amount of enthalpy per mole of H_2 taken out of the system by the exhaust stream containing the reaction products. The variables s_{in} and s_{out} are similar to h_{in} and h_{out}, respectively. All these variables can be determined by the following expressions:

$$h_{in} = \left(h_{H_2} + 0.5 \cdot h_{O_2} + 1.881 \cdot h_{N_2}\right)_{in}$$
$$h_{out} = \left(h_{H_2O} + 1.881 \cdot h_{N_2}\right)_{out} \tag{7}$$

$$s_{in} = \left(s_{H_2} + 0.5 \cdot s_{O_2} + 1.881 \cdot s_{N_2}\right)_{in}$$
$$s_{out} = \left(s_{H_2O} + 1.881 \cdot s_{N_2}\right)_{out} \tag{8}$$

Assuming ideal, nondissipative operation, the entropy generation is zero and substitution of eq. (6) into (5) gives the ideal power of the cell:

$$\dot{W}_{fc} = -\dot{N}_{H_2} \cdot \left(\Delta h - T_{fc} \cdot \Delta s\right) \tag{9}$$

where $\Delta h = h_{out} - h_{in}$ and $\Delta s = s_{out} - s_{in}$ represent the enthalpy and entropy change for the fuel cell reaction, respectively.

Inasmuch as the Gibbs free energy is given by $g = h - T \cdot s$, eq. (9) can be rewritten for isothermal operation:

$$\dot{W}_{fc} = \dot{N}_{H_2} \cdot (g_{in} - g_{out}) = -\dot{N}_{H_2} \cdot \Delta g \tag{10}$$

Notice that the previous equation is valid provided that the reactants and products streams are at the supposed temperature of operation of the cell. Since in this work the cell does not operate isothermally (reactants are at a lower temperature than the cell), eq. (10) is not valid and eq. (9) has been used to calculate the ideal power of the SOFC.

Once the ideal power is obtained, the maximum possible efficiency when the process is reversible can be formulated:

$$\eta_{fc} = \frac{W_{fc}}{-\dot{N}_{H_2} \cdot \Delta h} = \frac{\Delta h - T \cdot \Delta s}{\Delta h} \tag{11}$$

For the isothermal hydrogen and oxygen reaction to form gaseous water, the term Δs is lower than zero, indicating that heat is actually being lost from the fuel cell system. However, for the non-isothermal operation considered in this work, the temperature of the reactants is lower than that of the products and, under some conditions, the term Δs could be higher than zero. Under these circumstances, eq. (9) physically would indicate that the fuel cell absorbs heat from the ambient and converts it completely into electrical energy, with a fuel cell efficiency higher than unity. This is of course not possible, so operation at the supposed temperature of the cell is not achievable and the exit temperature of the products would be lower [9].

Finally, it is noted that, in this work, the enthalpy change (Δh) used in eqs. (9) and (11) is neither based on the higher heating value of the fuel nor on its lower heating value, but rather on the actual enthalpy change for the fuel cell reaction.

Absorption chiller model

The mathematical model of the absorption chiller is based on the application of global mass, species and energy balances and simple heat transfer equations. In formulating the model the following assumptions have been made: the refrigerant is considered pure water, heat losses to the environment are negligible, pressure drops are not considered, saturated solution conditions are assumed at the outlet of each of the four major components (absorber, desorber, condenser and evaporator), the temperature of the vapour leaving the desorber (state 7 in Figure 2) is the saturation temperature (T_{3eq}) corresponding to the pressure and concentration of the weak solution entering the desorber (state 3), and the pumping process is isoentropic.

For the solution heat exchanger a heat transfer model based on the effectiveness of the heat exchanger was used; then:

$$EFF_{ws-ss} = \frac{\max(T_3 - T_2, T_4 - T_5)}{T_4 - T_2} \quad (12)$$

For the generator, absorber, condenser and evaporator the heat transfer is expressed by the closest approach temperature (CAT):

$$CAT_G = \min(T_{12} - T_{3eq}, T_{11} - T_4) \quad (13)$$

$$CAT_A = \min(T_1 - T_{13}, T_6 - T_{14}) \quad (14)$$

$$CAT_C = \min(T_{7eq} - T_{16}, T_8 - T_{15}) \quad (15)$$

$$CAT_E = \min(T_{18} - T_9, T_{17} - T_{10}) \quad (16)$$

State equations used for the lithium bromide - water equilibrium and thermodynamic properties have been calculated from McNeely [10]. The crystallization temperature was calculated with the formulations of Pátek and Klomfar [11]. The remainder model equations are not presented here for the sake of brevity, but they are described in detail for similar systems in [12, 13].

The mathematical model has been used to determine the thermodynamic state and the mass flow rates at every representative point in the thermodynamic cycle of the absorption system, as well as the heat flux in each heat exchanger ($\dot{Q}_G$, $\dot{Q}_A$, $\dot{Q}_C$, $\dot{Q}_E$ and $\dot{Q}_{ws-ww}$) and the power required by the pump ($\dot{W}_p$). The absorption system coefficient of performance is obtained from eq. (17).

$$COP = \frac{\dot{Q}_E}{\dot{Q}_G + \dot{W}_p} \quad (17)$$

Efficiency of the combined system

The energy utilization coefficient for the combined system is defined as the ratio of the useful energy extracted from the system (electrical, cooling and hot water production) to the energy of the fuel input (based on its higher heating value):

$$PER = \frac{\dot{Q}_E + \dot{W}_{fc} + \dot{Q}_{hw}}{\dot{N}_{H_2} \cdot HHV_{H_2}} \quad (18)$$

RESULTS AND DISCUSSION

The mathematical model described in the previous section has been programmed using Engineering Equation Solver (EES) [14]. The model has been used to simulate and analyze the performance of an integrated hydrogen fuel cell with a LiBr-water absorption system for combined production of electricity, cooling and hot water. The input parameters and operating conditions considered for the analysis are indicated in Table 1. The input data have been divided into three groups: the integration system data, specific data for the SOFC and specific data of the absorption chiller.

Table 1. Operating conditions.

Parameters	Values
Integrated system	
Fuel composition	H_2 100%
Air composition	O_2 21%, N_2 79%
Inlet temperature of fuel and air ($T_1 = T_3$)	25 ºC
Operating pressure	100 kPa
Gases temperature variation to power absorption chiller ($\Delta T = T_{10} - T_{11}$)	25 ºC
Domestic hot water inlet temperature (T_{13})	15 ºC
Domestic hot water outlet temperature (T_{14})	60 ºC
Hot water heat exchanger efficiency (EFF_{hw})	0.9
SOFC	
Fuel utilization ratio	100%
Operating temperature (T_{fc})	900 ºC
Operating pressure	100 kPa
Absorption chiller	
Generation temperature (T_4)	95 ºC
Chilled water inlet temperature (T_{17})	12 ºC
Chilled water outlet temperature (T_{18})	7 ºC
Condenser/absorber cooling water inlet temperature ($T_{13} = T_{15}$)	30 ºC
Condenser/absorber cooling water outlet temperature ($T_{14} = T_{16}$)	35 ºC
Closest approach temperature (CAT) in heat exchangers	5 ºC
Solution heat exchanger efficiency (EFF_{ws-ss})	0.9
Pump isoentropic efficiency	1

Tables 2 and 3 show the direct results of the integrated system and absorption system, considering the data in Table 1 and a fuel molar flow rate of 1 mol/s.

It is known that for an absorption system, the COP increases with increasing values of the evaporating temperature and decreasing values of the absorption/condensation temperatures. The evaporating temperature depends on the cooling water temperature required for a given application and on the difference between the cooling water and refrigerant temperatures in the evaporator (CAT_E). The first one is a system operating parameter and the second one is a heat transfer design parameter of the evaporator. Similarly, the absorption/condensation temperatures depend on the external sink temperature (usually water from a cooling tower) and the closest approach temperatures in both components. It is then

clear that for a given application the value of the *CAT* of the different components should be reduced to a minimum for a COP optimization.

Table 2. Thermo-fluid properties at each point of the integrated system

	T (ºC)	$\dot{N}$ (mol/s)	Composition (mol%)	
1	25	1	H2: 100%	
2	770	1	H2: 100%	
3	25	2.381	O2: 21%	N2: 79%
4	770	2.381	O2: 21%	N2: 79%
5	900	2.881	H2O: 34.7%	N2: 65.3%
6	900	0.8215	H2O: 34.7%	N2: 65.3%
7	109	0.8215	H2O: 34.7%	N2: 65.3%
8	900	2.059	H2O: 34.7%	N2: 65.3%
9	109	2.059	H2O: 34.7%	N2: 65.3%
10	109	2.881	H2O: 34.7%	N2: 65.3%
11	84	2.881	H2O: 34.7%	N2: 65.3%
12	22	2.881	H2O: 34.7%	N2: 65.3%
13	15	1.61	H2O(l): 100%	
14	60	1.61	H2O(l): 100%	

Table 3. Calculated parameters of the integration system (per mol/s of H_2).

Parameters	Values
SOFC	
Enthalpy change for the fuel cell reaction (Δh)	-234409 (kJ/kmol)
Entropy change for the fuel cell reaction (Δs)	-37.9 (kJ/kmol·K)
Electric power ($\dot{W}_{fc}$)	190 kW
Heat transfer rate to the ambient ($\dot{Q}_{fc}$)	444.4 kW
Fuel cell efficiency (η_{fc})	0.81
Absorption chiller	
Evaporation/absorption pressure	0.71 kPa
Condensation/generation pressure	7.38 kPa
Strong solution concentration	0.646
Weak solution concentration	0.575
Cooling power ($\dot{Q}_E$)	1.75 kW
COP	0.787
Integrated system	
HHV_{H_2}	285830 kJ/kmol
H_2 heat exchanger efficiency (EFF_{H_2})	0.905
Air heat exchanger efficiency (EFF_{air})	0.905
Hot water heating power ($\dot{Q}_{hw}$)	5.46 kW
PER	0.690

The performance of the absorption cycle is also influenced by the generation temperature. Differing from the other three temperatures which are practically fixed for a given application, the generation temperature can be selected as long as its value is lower than the heat source temperature level.

Figure 3 shows the effect of the generation temperature on the absorption system COP, the absorber inlet temperature and the crystallization temperature at the absorber inlet conditions (strong solution concentration and absorber pressure). It can be seen that when the generation temperature increases from 84 to 100 ºC, the COP varies from a low value of 0.76 (it drops

sharply for lower values of the generation temperature) to values of around 0.785. However, for generation temperature values higher than 95 ºC the COP curve is relatively flat. With respect to the absorber inlet temperature and the crystallization temperature, Figure 3 shows that the first one increases gently with the generation temperature, but the second one is highly influenced by the generation temperature. This sharp increase of the crystallization temperature is due to the increase of the strong solution concentration with the generation temperature. It can be seen that for generation temperatures lower than 97 ºC the crystallization temperature is lower than the absorber inlet temperature.

The temperature range shown in the Figure 3 spans the practical generation temperatures for this application. For generation temperatures lower than 84 ºC the cycle operation is not possible and for values higher than 97 ºC crystallization occurs. The generation temperature value of 95 ºC that was chosen (see Table 1) leads to good COP values with a small margin to avoid crystallization.
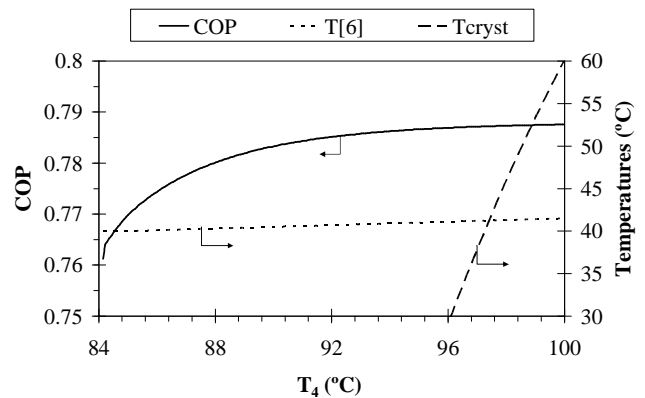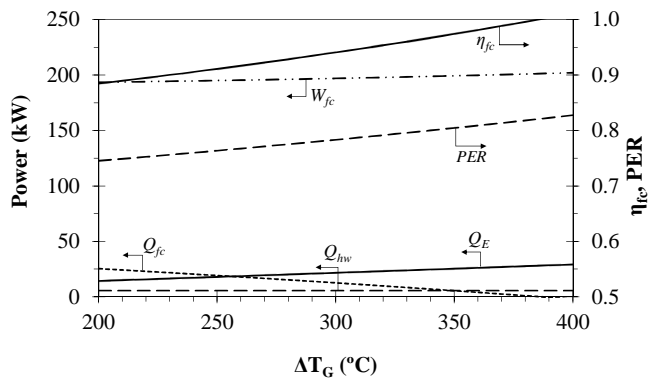

Figure 3 Effect of the generation temperature on COP, absorber inlet temperature and crystallization temperature at the absorber inlet conditions.

Figure 4 shows the effect of the gases temperature variation to power the absorption chiller ($\Delta T_G = T_{10} - T_{11}$) on the system performance, considering a fuel molar flow rate of 1 mol/s. It can be seen that when increasing the gases temperature variation to power the absorption chiller, the electric power of the SOFC and the cooling power delivered by the absorption chiller increase, while the hot water heating power remains constant. Figure 4 also shows that when ΔT_G increases, the fuel cell efficiency increases from 88% to 100% and the PER of the system increases from 74% to 82%.

When ΔT_G increases the temperature of the reactants at the inlet of the SOFC decreases, as a result the enthalpy ($-\Delta h$) and entropy ($-\Delta s$) changes for the fuel cell reaction decreases. Since the variation of ($-T_{fc}\cdot\Delta s$) is higher than that of ($-\Delta h$), the heat released from the fuel cell to the surroundings decreases and the ideal power of the cell increases until a 100% efficiency is reached. These particular conditions are for a reversible adiabatic operation of the fuel cell. In this analysis, increasing

ΔT_G leads to higher values of PER because it is assumed that the heat released from the fuel cell is dissipated to the ambient.

Figure 4 Effect of the of the gases temperature variation to power absorption chiller (ΔT_G) on the system performance, considering a fuel molar flow rate of 1 mol/s.

CONCLUSION

In this paper a mathematical model has been developed to simulate an integrated hydrogen fuel cell with a LiBr-water absorption system for the combined production of electricity, cooling and hot water. The program and the mathematical model are divided into three modules: SOFC module, absorption chiller module and the integrated system module. Given the typical operating temperature conditions for SOFCs, domestic hot water demands and a LiBr-water absorption chiller, the performance of the integrated system can be evaluated. Once these temperature levels are fixed, the effect of the absorption system generation temperature and the gases temperature variation to power the absorption chiller can be scrutinized in order to determine optimum operating conditions. It was shown that a generation temperature value of 95 ºC leads to a high COP value with a small margin to avoid crystallization. On the other hand, it was shown that increasing the gases temperature variation to power the absorption chiller results in higher electric powers, higher cooling powers and constant domestic hot water heating powers. The energy utilization coefficient for the integrated system (PER) is expected to reach a maximum value of around 82% for reversible adiabatic operation of the fuel cell.

REFERENCES

[1] Conte M., Iacobazzi A., Ronchetti M., and Vellone R., Hydrogen economy for a sustainable development: state-of-the-art and technological perspectives, *Journal of Power Sources*, Vol. 100, 2001, pp. 171-187.

[2] Zink F., Lu Y., and Schaefer L., A solid oxide fuel cell system for buildings, *Energy Conversion and Management*, Vol. 48, 2007, pp. 809–818

[3] Al-Sulaiman F.A., Dincer I., and Hamdullahpur F., Energy analysis of a trigeneration plant based on solid oxide fuel cell and organic Rankine cycle, *International Journal of Hydrogen Energy*, Vol. 35, 2010, pp. 5104-5113.

[4] Pilatowsky I., Romero R.J., Isaza C.A., Gamboa S.A., Rivera W., Sebastian P.J., and Moreira J., Simulation of an air conditioning absorption refrigeration system in a co-generation process combining a proton exchange membrane fuel cell, *International Journal of Hydrogen Energy*, Vol. 32, 2007, pp. 3174-3182.

[5] Baniasadi E., Alemrajabi A.A., Fuel cell energy generation and recovery cycle analysis for residential application, *International Journal of Hydrogen Energy*, Vol. 35, 2010, pp. 9460-9467.

[6] Braun R.J., Klein S.A., Reindl D.T., Evaluation of system configurations for solid oxide fuel cell-based micro-combined heat and power generators in residential applications, *Journal of Power Sources*, Vol. 158, 2006, pp. 1290-1305.

[7] Chase M.W., NIST-JANAF thermochemical tables, 4th Edition, *Journal of Physical and Chemical Reference Data,* 1998.

[8] Li X., Thermodynamic Performance of Fuel Cells and Comparison with Heat Engines, in: Zhao T.S., Kreuer K.D., Nguyen T.V. (Eds.), Advances In Fuel Cells, Elsevier, Oxford, 2007.

[9] Gaggioli M.W., and Dunbar W.R., Emf, maximum power and efficiency of fuel cells, *Energy Resources and Technology*, Vol. 115, 1993, pp. 100-104.

[10] McNeely L.A., Thermodynamic properties of aqueous solutions of lithium bromide, *ASHRAE Transactions*, Vol. 85 Part 1, 1979, pp. 413-434.

[11] Pátek J., and Klomfar J., Solid liquid phase equilibrium in the systems of LiBr/H$_2$O and LiCl/H$_2$O, *Fluid Phase Equilibria*, Vol. 250 (1-2), 2006, pp. 138-149.

[12] Herold K.E., Radermacher R., and Klein S.A., Absorption chillers and heat pumps, CRC Press, Boca Ratón, Florida, 1996.

[13] Fernández-Seara J., and Sieres J., Ammonia-water absorption refrigeration systems with flooded evaporators, *Applied Thermal Engineering*, Vol. 26, 2006, pp. 2236-2246.

[14] Klein S.A., Engineering Equation Solver (EES), F-Chart Software, Middleton, WI, 1992-2006.